
Future Satellite Gravity Field Missions: Feasibility Study of Post-Newtonian Method **28**

R. Mayrhofer and R. Pail

Abstract

Modern satellite gravity field recovery missions use accelerometric, intersatellite tracking or gradiometric observables for deducing gravity field related data. In this study an alternative observable type for gravity field recovery, the relativistic frequency shift, is investigated. As Einstein stated in his general theory of relativity, gravity can be considered as attribute of space-time. In this view mass alters the geometric shape of the metric tensor. Moreover mass, respectively gravity, has effects on electromagnetic wave propagation [Einstein (Annalen der Physik 35:898–908 1911)]. Although these relativistic effects are quite small and difficult to measure, with upcoming atomic clocks which have sufficient accuracy and short-term stability it will be possible to derive meaningful gravity related information. Since relativistic effects are used this method is called Post-Newtonian method. The main target of this paper is to demonstrate the validity of the derived relativistic equations.

The scientific quality of the relativistic frequency shift observed by means of highly accurate atomic clocks is investigated. In our basic scenario a low earth orbit (LEO) sends an electromagnetic wave to a receiver. The reference station determines the frequency shift of the signal, which is connected to the time dilatation between the atomic clock of the satellite and an identical atomic clock nearby the receiver. A simplified, mathematical model for numerical simulations of this configuration is presented. The effect of different error sources are investigated by numerical closed-loop simulations. Thus, the performance requirements of atomic clocks, position and velocity determination and limiting factors for deducing earth's gravity field can be derived.

28.1 Introduction

In this study the principle of the Post-Newtonian method for earth gravity field determination is presented. The observable for gravity field reconstruction is the frequency shift of an electromagnetic signal transmitted from a satellite to a receiver station. This frequency shift is caused by relativistic time dilatation

R. Mayrhofer (✉) • R. Pail
Institute of Navigation and Satellite Geodesy, Graz University
of Technology, Steyrergasse 30, 8010 Graz, Austria
e-mail: reinhard.mayrhofer@tugraz.at

which is related to the gravity potential. By numerical simulations the spatial and spectral performance of a LEO satellite mission equipped with atomic clocks, which will be available within the next tow decades, is investigated.

There have been done some studies which are related to future satellite gravity field missions and general relativistic effects. There is for example the Einstein Gravity Explorer mission proposal (Schiller et al. 2009) in which testing methods of relativistic effects and physical constants based on atomic clock measurements are investigated. Müller et al. (2007) explored the impact of relativity on various geodetic topics like the geoid, reference systems, geodynamics, Global Positioning System (GPS), Satellite Laser Ranging (SLR), and Very Long Base Interferometry (VLBI). Gulkett (2003) investigated relativistic effects on GPS and LEO and showed how to implement them correctly within a relativistic framework. The IAU already included relativistic effects for frame transformations (Soffel et al. 2003).

For being able to realise a satellite mission as proposed in this paper, atomic clocks with sufficient quality will be needed. Actual atomic clocks achieve a short term stability of 10^{-16} s (between two measurement epochs) on earth (Schiller 2007) and are expected to achieve 10^{-18} s within the next 15 years. According to Cacciapuoti (2006), actual space-borne atomic clocks achieve an accuracy of 10^{-15} s. Thus, a satellite mission with an atomic clock with 10^{-18} s stability should be possible within the next 30 years.

In this study, the equations for the Post-Newtonian method are derived in Chaps. 28.2 and 28.3. In Chap. 28.4 the simulation setup is described in more detail. Chapter 28.5 shows the simulation results, a performance analysis, and the analysis of the spectral and spatial error behaviour. Finally a conclusion and outlook is given in Chaps. 28.6 and 28.7.

28.2 Relativistic Time Dilation

The metric tensor $g_{\mu\nu}$ describes the curvature of space-time. Thus, it can be used for deducing a description of the relativistic frequency shift. The line element ds can be described by

$$ds^2 = g_{\mu\nu}(x)dx^\mu dx^\nu \quad (28.1)$$

Here Einstein's tensor convention has been applied (Einstein 1916). Double upper and lower indices describe a summation. The gradient $dx^\kappa = [-c \cdot dt \ dx^1 \ dx^2 \ dx^3]^T$ of the scalar vector field $x = (x^\kappa)$ contains position and time information. c is the speed of light in vacuum, dt the time element of a chosen time system and dx^i describe the three dimensional coordinate elements. The metric tensor $g_{\mu\nu}(x)$ is a function of x^κ ($\mu, \nu, \kappa = [0, 1, 2, 3]$), which means that the curvature of space-time depends on time and position.

A solution of Einstein's field equations delivers the elements of the metric tensor. A series expansion representation of the tensor elements is (Soffel et al. 2000)

$$\begin{aligned} g_{00} &= -1 + \frac{2 \cdot \Phi(x)}{c^2} - \frac{2 \cdot \Phi^2(x)}{c^4} + O(c^{-5}) \\ g_{0i} &= -\frac{4 \cdot \Phi^i(x)}{c^3} + O(c^{-5}) \\ g_{ij} &= \delta_{ij} \left(1 + \frac{2 \cdot \Phi(x)}{c^2} - \frac{2 \cdot \Phi^2(x)}{c^4} \right) + O(c^{-6}) \end{aligned} \quad (28.2)$$

where $\Phi(x)$ is the gravity potential and $i, j = [1, 2, 3]$. The earth's static gravity field potential is usually expressed by a spherical harmonic series expansion (Heiskanen and Moritz 1967):

$$\begin{aligned} \Phi_E(r, \theta, \lambda) &= \frac{GM}{R} \cdot \sum_{l=0}^{\infty} \left(\frac{R}{r} \right)^{l+1} \cdot \\ &\sum_{m=0}^l (\bar{C}_{lm} \cos m\lambda + \bar{S}_{lm} \sin m\lambda) \cdot \bar{P}_{lm}(\cos \theta) \end{aligned} \quad (28.3)$$

Here r , θ and λ are spherical coordinates, R is the earth's reference radius, GM the gravitational constant times mass of the earth, l and m are the degree and order of the fully normalized spherical coefficients \bar{C}_{lm} , \bar{S}_{lm} , and $\bar{P}_{lm}(\cos \theta)$ represents the fully normalized Legendre function. Equation (28.3) describes the functional model for setting up the design matrix for least squares adjustment in our simulation environment. The spherical coefficients \bar{C}_{lm} , \bar{S}_{lm} are the system parameters, while the gravity potential Φ , which is derived from relativistic frequency shifts is the observable of our system.

The local line element ds_{clock} of a clock moving within a gravity field affects the displayed time $d\tau_{clock}$ and frequency ν_{clock} of the clock.

$$d\tau_{clock} = \frac{1}{\nu_{clock}} = \frac{ds_{clock}}{c} = \frac{1}{c} \sqrt{g_{\mu\nu}(x) dx^\mu dx^\nu} \quad (28.4)$$

$x = (x^k)$ and dx^k are related to the coordinates of the clock. The coordinate elements of a moving clock can be described by

$$dx^k = [-c \cdot dt \quad v^1 dt \quad v^2 dt \quad v^3 dt] \quad (28.5)$$

Here, $v^i = v^i(x)$ denotes the velocity of the clock and is related to its coordinates, too. Merging (28.2), (28.4) and (28.5) and omitting elements smaller than c^{-3} leads to a description of the inherent time of a moving body:

$$d\tau^2 = \left[-1 + \frac{2 \cdot \Phi(x)}{c^2} + \frac{v_*^2(x)}{c^2} \right] \cdot dt^2 \quad (28.6)$$

$v_*(x)$ is the local scalar velocity of the clock. The asterisk ‘*’ is used for underlining that v is scalar and preventing to mix it up with the velocities from (28.5). dt represents a virtual time of an non-moving, gravity-free (inertial) body located at infinite distance.

28.3 Functional Model

A LEO satellite transmits an electromagnetic signal via microwave link to a receiver station. This receiver station could be a geostationary satellite or a reference station located on earth’s surface. By comparing the local frequency of the transmitted signal with the local frequency of the received signal the time dilation between receiver and transmitter is defined. By using (28.6) and again omitting elements smaller than c^{-3} the ratio of receiver and transmitter frequency is obtained by

$$\begin{aligned} \Delta\nu_{RT} &= \frac{\nu_R}{\nu_T} = \frac{d\tau_T}{d\tau_R} \\ &= \sqrt{\frac{-1 + \frac{2 \cdot \Phi_T}{c^2} + \frac{v_{T*}^2}{c^2}}{-1 + \frac{2 \cdot \Phi_R}{c^2} + \frac{v_{R*}^2}{c^2}}} + O(c^{-4}) \end{aligned} \quad (28.7)$$

The lower indices R and T describe a receiver, respectively a transmitter related variable. The gravity

potentials are related to the receiver or transmitter position $\Phi_R = \Phi(x_R^k)$, $\Phi_T = \Phi(x_T^k)$. This equation is used for synthesizing relativistic frequency shifts in our simulation environment. Moreover it is the fundamental equation for the Post-Newtonian approach. As the relativistic time dilation, which is not modeled by the Newtonian framework, is taken into account, the nomenclature ‘Post-Newtonian’ has been chosen to describe this method. The gravity potential Φ_T deduced from the frequency shift $\Delta\nu_{RT}$ is the prime observable for the Post-Newtonian method. A general description of (28.7) is

$$\Delta\nu_{RT} = \frac{\nu_R}{\nu_T} = \frac{d\tau_T}{d\tau_R} = \sqrt{\frac{g_{\mu\nu}(x_T) dx_T^\mu dx_T^\nu}{g_{\mu\nu}(x_R) dx_R^\mu dx_R^\nu}} \quad (28.8)$$

By combining (28.8) with the description of the metric tensor elements in (28.2), (28.7) can be achieved. Based on this function the gravity potential Φ_T at the satellite position can be calculated from a measured frequency shift $\Delta\nu_{RT}$. After some reformulations a function, which is used in our simulation environment as functional model for deducing the gravity potential at transmitter position from the frequency shift $\Delta\nu_{RT}$, is achieved:

$$\Phi_T = \left[\Delta\nu_{RT}^2 \cdot \Omega_R - \frac{v_{T*}^2}{c^2} + 1 \right] \cdot \frac{c^2}{2} \quad (28.9)$$

Here a support variable Ω_R has been introduced. It contains all position, velocity and gravity potential information of the receiver station:

$$\Omega_R = -1 + \frac{2 \cdot \Phi_R}{c^2} + \frac{v_{R*}^2}{c^2}.$$

Equations (28.9) and (28.10) describe two relativistic effects. The first one is time dilation caused by relative movement of receiver and transmitter, the second one time dilation caused by the gravity potential difference between transmitter and receiver location.

The gravity potential $\Phi(x)$ is composed of all occurring gravity potentials. As a first approximation in our simulations, all non-earth gravity potentials and tide signals have been neglected. Beside the special relativistic and general relativistic effects the Doppler shift is the third large effect which influences the

frequency observations of the receiver station. As a satellite in a LEO achieves large velocities, the radial velocity between receiver and transmitter cause a Doppler frequency shift which has to be modeled. The Doppler shift (Doppler 1842) is defined by

$$v_R = v_T \sqrt{\frac{c - v_{TR}^*}{c + v_{TR}^*}} \quad (28.10)$$

where v_{TR}^* is the scalar radial velocity between transmitter and receiver. The Doppler shift is applied to the measured frequency at the receiver station. It has to be mentioned that as we are working in a relativistic framework, the radial velocity has to be derived in a coordinate system located at the center of the receiver station.

28.4 Simulation Setup

Figure 28.1 shows the schematic set-up of our simulation software. In a configuration file the orbit properties, computation switches and observation noise types are defined. The software computes based on this configuration, the orbit positions and the frequency related effects by using (28.7) and (28.10). In our simulation environment (28.9) has been used to calculate the gravity potential at the satellite position from the synthesized frequency shifts.

The simulation environment has been designed to determine the influence of data noise on the reproduced gravity field model. Therefore it is possible to manually add realistic noise on frequency and velocity measurements. Following effects on the frequency shift observable have been simulated:

- Special relativistic frequency shift caused by relative velocity of receiver and transmitter clock (28.7).
- General relativistic frequency shift caused by relative potential difference at receiver and transmitter clock positions (28.7).
- Doppler Effect caused by relative radial velocity of receiver and transmitter clock (28.10).

For every effect a realistic stochastic noise signal was added on noise-free frequency and velocity measurements. Shin et al. (2008) suppose a coloured noise for H-maser clocks with increasing amplitudes at low and high frequencies and linear behaviour in-between.

Figure 28.2 shows the power spectrum density function of the atomic clock noise with amplitude 10^{-17} and 10^{-18} s generated for our simulations based on this information. For the velocity error, white noise has been assumed.

In the frame of gravity field adjustment, the stochastic models, which define the metric of the normal equation system, have been consistently incorporated by correspondingly designed digital filters applied to both, the observation time series and the columns of the design matrix (Schuh, 2001).

A nearly polar (89.5° inclination), circular repeat orbit with 25 days and 403 cycles at 300 km mean height with 10 s sampling interval has been chosen for all simulations.

28.5 Simulation Results

28.5.1 Performance Analysis

The main observable of the Post-Newtonian method is the frequency shift. Equation (28.7) shows that beside the atomic clock noise the velocity determination noise

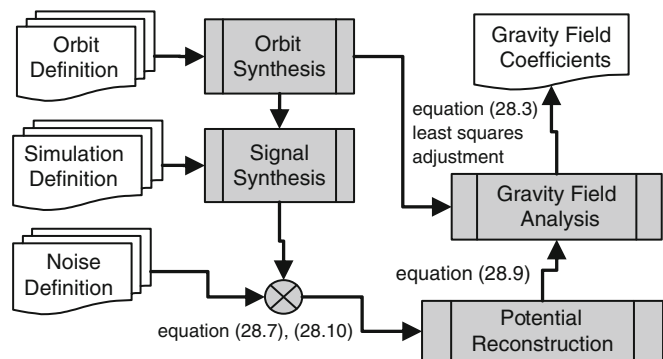


Fig. 28.1 Schematic presentation of the simulation environment used in this study

Fig. 28.2 Smoothed noise amplitude spectrum of coloured clock noise with amplitude 10^{-17} s and 10^{-18} s

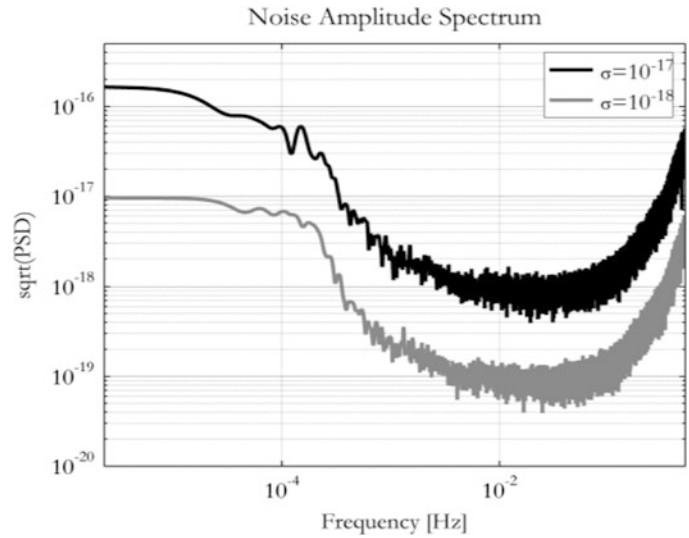
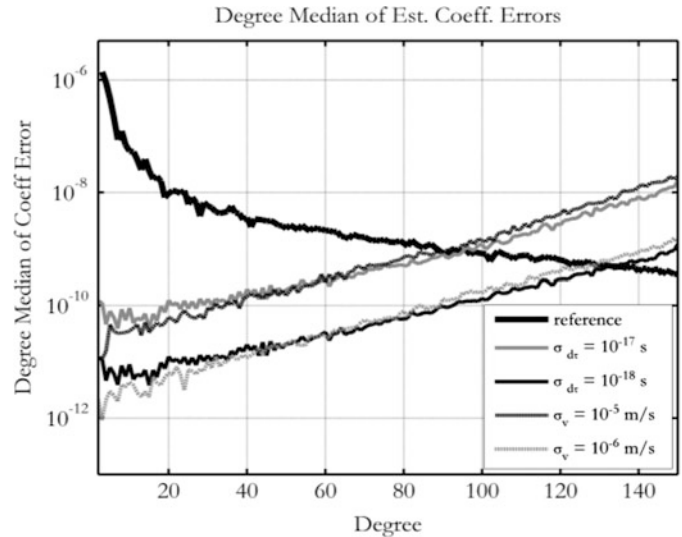


Fig. 28.3 Degree error median plot of simulations with frequency noise with 10^{-17} s and 10^{-18} s amplitude and velocity noise with 10^{-5} m/s and 10^{-6} m/s white noise



of the transmitter is a stochastic variable, too and is the second limiting factor for the Post-Newtonian method.

Based on the frequency shift the transmitter potential can be determined by using (28.10). Thus, first a noise free data set has been defined, and the calculation method has been verified by using closed-loop computations. Next, realistic coloured clock noise (Fig. 28.2) with amplitudes of 10^{-16} up to 10^{-18} s has been applied to the synthetic observations. Finally, signals including white velocity noise at amplitudes of 10^{-4} to 10^{-6} m/s have been used instead.

Figure 28.3 shows the degree error median of the by least squares adjustment reproduced gravity field

coefficients up to d/o (degree and order) 150. It can be seen that the velocity noise of 10^{-5} m/s has an effect on the gravity field reconstruction error which is comparable to 10^{-17} s clock noise, while 10^{-6} m/s velocity noise has a similar influence as 10^{-18} s clock noise.

Moreover it can be seen that future atomic clocks (Cacciapuoti 2006; Schiller 2007) with an expected short term stability of 10^{-18} s clock noise, and positioning precision of 10^{-6} m/s velocity noise it would be possible to deduce earth's gravity field up to d/o 120. It has to be mentioned that following effects, which will in practice have additional contributions on the total error budget, have been neglected in our simulations:

- Tidal and non-tidal temporal variable effects.
- Non-conservative potentials
- Relativistic effects on frame transformations.
- Non-uniformly rotating earth.
- Non-inertial potentials (satellite rotation).
- Receiver position related errors (position, velocity and the gravity potential at receiver position are assumed to be error-free).
- Dispersive atmosphere related effects.

However, it can be expected that the error terms included in this study are the dominant ones.

28.5.2 Spatial and Spectral Error Structure

As the gravity potential at the transmitter position, which is deduced from frequency measurements, is the observable for the least squares adjustment, the error structure of the recovered earth gravity field corresponds to the error structure of direct potential observations. Thus, in the case of white noise, the error amplitude increases with higher degree and order of deduced spherical coefficients and the slope of the degree error median is related to the chosen orbit height. Figure 28.4

Fig. 28.4 Geoid height error of simulation with 10^{-18} s clock noise applied on frequency observations. A homogeneous and isotropic error structure is provided

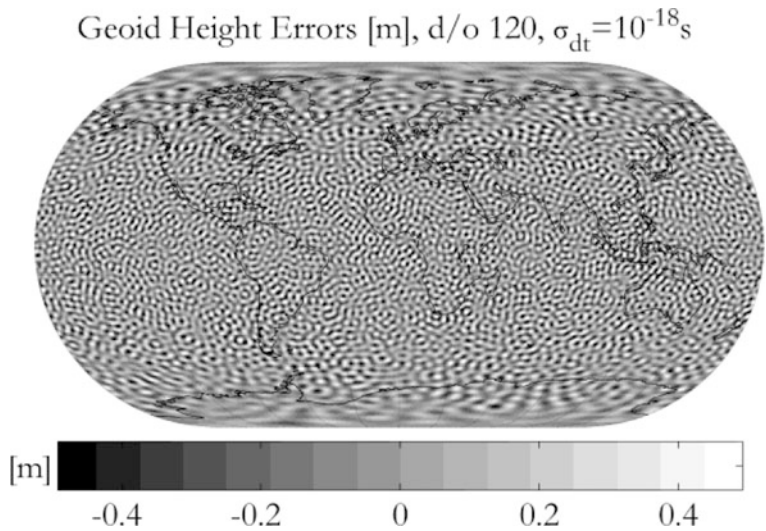
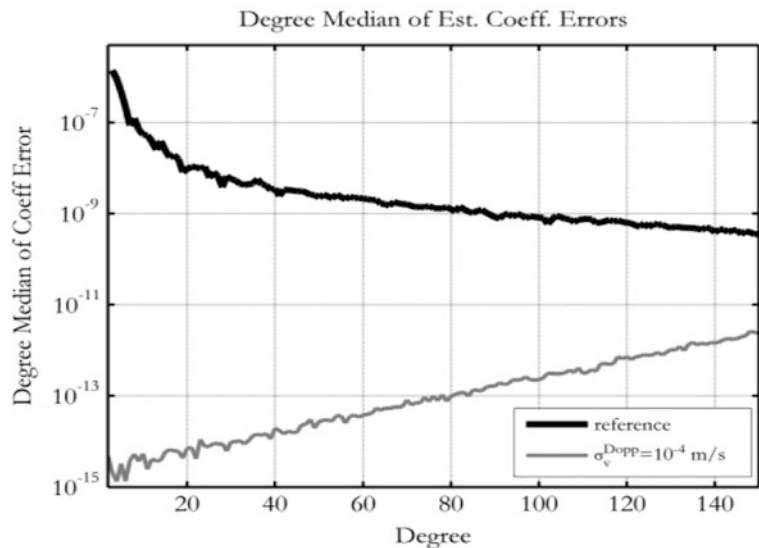


Fig. 28.5 Degree error median plot of Doppler velocity error with 10^{-4} m/s noise simulation. Compared to the simulations shown in Fig. 28.3 the influence of Doppler noise is negligibly small



shows the homogeneous and isotropic spatial error distribution of a simulation configuration with 10^{-18} s clock noise. Simulations with white velocity noise superposed show similar spatial error structures.

28.5.3 Doppler Shift

A simulation setup has been defined, where the Doppler shift has been applied on synthetic frequency observations based on noise-free data with which relativistic influences were modeled before. White noise with amplitude of 10^{-4} m/s has been superposed on the noise-free velocities (28.10).

Figure 28.5 shows that the Doppler shift can be modeled very well even at high velocity noise amplitudes. Moreover, the influence on the recovered gravity field is negligibly small up to d/o 250. So the Doppler shift is no limiting factor. The reason for this is because compared to (28.9), the radial velocity in (28.10) is not scaled by c^2 .

28.6 Conclusions

It has been shown that the Post-Newtonian method is a feasible method for reproducing earth's gravity field for lower and medium frequencies, provided that the technological development of space-borne atomic clocks proceeds in the future. Additionally it has been shown that the derived equations are valid within the defined mission scenario. The two dominant error contributions of this method are the atomic clock noise and the satellite velocity error of the precise orbit determination. The Doppler-effect, which also influences the frequency measurements, can be modeled with sufficient precision, so its error does not leak into the recovered gravity coefficients. It has to be mentioned that the simulations done here should be seen as a concept study and some more realistic simulations will be done to provide more information about the behaviour of the method.

A velocity determination precision up to 10^{-6} m/s and an atomic clock short term stability of 10^{-18} s is required to resolve the gravity field up to d/o 120. The main advantage of this method is its homogeneous and isotropic spatial error structure.

28.7 Outlook

With upcoming atomic clocks below 10^{-16} s short term stability and improving positioning and velocity determination methods, the presented method can be an additional piece for a global earth gravity field monitoring framework in a not too far future. Beside the single-satellite mission presented in this study, various satellite constellations and formations can be designed. In what extent satellite formations like Pendulum, Cartwheel or LISA-like lead to improved precision still has to be investigated by numerical simulations. There is no doubt that multi-satellite missions would underline the possible power of the Post-Newtonian method.

One, two or three geostationary satellites could be used as reference stations. Additional rover satellites could be placed in different orbit types. A dense network of satellites could improve the time resolution, so the time variable gravity field could be optimally mapped. These satellites could be equipped with two or more RF-antennas, so one satellite could establish a connection to two or more other satellites, which would further increase the measurement density of the network.

As the equations used in this study are strongly simplified, the influences of other effects have to be further investigated. First real orbits and non-conservative forces have to be modeled. Next, the influence of satellite rotation has to be investigated. Additional attitude information from star-tracker measurements and its noise behaviour have to be simulated. All observations and calculations have to be done in a relativistic framework. So the influences of frame transformations in this relativistic framework have to be investigated.

All other effects listed in Chap. 28.5.1 will be further investigated in upcoming simulations. This will lead to a much more complex mathematical description which will be harder to linearize, but will also be closer to reality. The main target of upcoming simulations will be to set up a more realistic environment and to design multi-satellite missions that support the advantages of the Post-Newtonian method. Moreover there will be done simulations concerning the time variable gravity field. It will be investigated how different mission design affects the quality of the static and time variable gravity field and if there is

a possibility to deduce models with higher spatial and temporal resolution.

Acknowledgements We would like to thank L. Vitushkin and an anonymous reviewer for their valuable comments which helped to improve the manuscript.

References

- Cacciapuoti L (2006) Atomic Clocks in Space. *ESA-ESTEC (SCI-SP)*, Frascati
- Doppler C (1842) Ueber das farbige Licht der Doppelsterne und einiger anderer Gestirnen des Himmels. *Abhandlungen der k. böhm. Gesellschaft der Wissenschaften Folge V Band 2*, In Commision bei Borrosch & André, Prag
- Einstein A (1911) Über den Einfluß der Schwerkraft auf die Ausbreitung des Lichtes. *Annalen der Physik* 35, Verlag von Johann Ambrosius Barth, Leipzig pp 898–908
- Einstein A (1916) Die Grundlage der allgemeinen Relativitätstheorie. *Annalen der Physik* 49, Verlag von Johann Ambrosius Barth, Leipzig pp 769–821
- Gulkett M (2003) Relativistic effects in GPS and LEO. Rapport for the Cand. Scient. degree, University of Copenhagen, Department of Geophysics, The Niels Bohr Institute for Physics, Astronomy and Geophysics, Denmark
- Heiskanen WA, and Moritz H (1967). *Physical Geodesy*. W. H. Freeman & Co Ltd, San Francisco, ISBN-13 978-0716702337
- Müller J, Soffel M and Klioner SA (2007) Geodesy and relativity. *Journal of Geodesy* 82 Number 3, Springer, Berlin, ISSN 0949-7714, pp 133–145
- Schiller S (2007) Gravimetry with optical clocks. Workshop on The Future of Satellite Gravimetry 12–13 April 2007, ESTEC
- Schiller S, Tino GM, Gill P, Salomon C, Sterr U, Peik E, Nevsky A, Görlitz A, Svehla D, Ferrari G, Poli N, Lusanna L, Klein H, Margolis H, Lemonde P, Laurent P, Santarelli G, Clairon A, Ertmer W, Rasel E, Müller J, Iorio L, Lämmerzahl C, Dittus H, Gill E, Rothacher M, Flechner F, Schreiber U, Flambaum V, Ni, Wei-Tou, Liu, Liang, Chen, Xuzong, Chen, Jingbiao, Gao, Kelin, Cacciapuoti L, Holzwarth R, Heß MP, Schäfer W (2009) Einstein gravity explorer – a medium class fundamental physics mission. *Exp Astron* 23 (2):573–610
- Shin MY, Park C and Lee SJ (2008) Atomic Clock Error Modeling for GNSS Software Platform. Position, Location and Navigation Symposium, IEEE/ION Plans 2008, pp 71–76, 1-4244-1537-03/08
- Schuh W-D (2001) Improved modeling of SGG-data sets by advanced filter strategies. ESA-Project (Hg.): From Eötvös to mGal+, WP2, Midterm-Report, pp 113–181
- Soffel M, Klioner A, Petit G, Wolf P, Kopeikin SM, Bretagnon P, Brumberg VA, Capitaine N, Damour T, Fukushima T, Guinot B, Huang T-Y, Lindgren L, Ma C, Nordtvedt K, Ries JC, Seidelmann PK, Vokrouhlicky D, Will CM, Xu C (2003) The IAU 2000 resolution for astrometry, celestial mechanics, and metrology in the framework: explanatory supplement. *Astron J* 126:2687–2706, The American Astronomical Society. USA